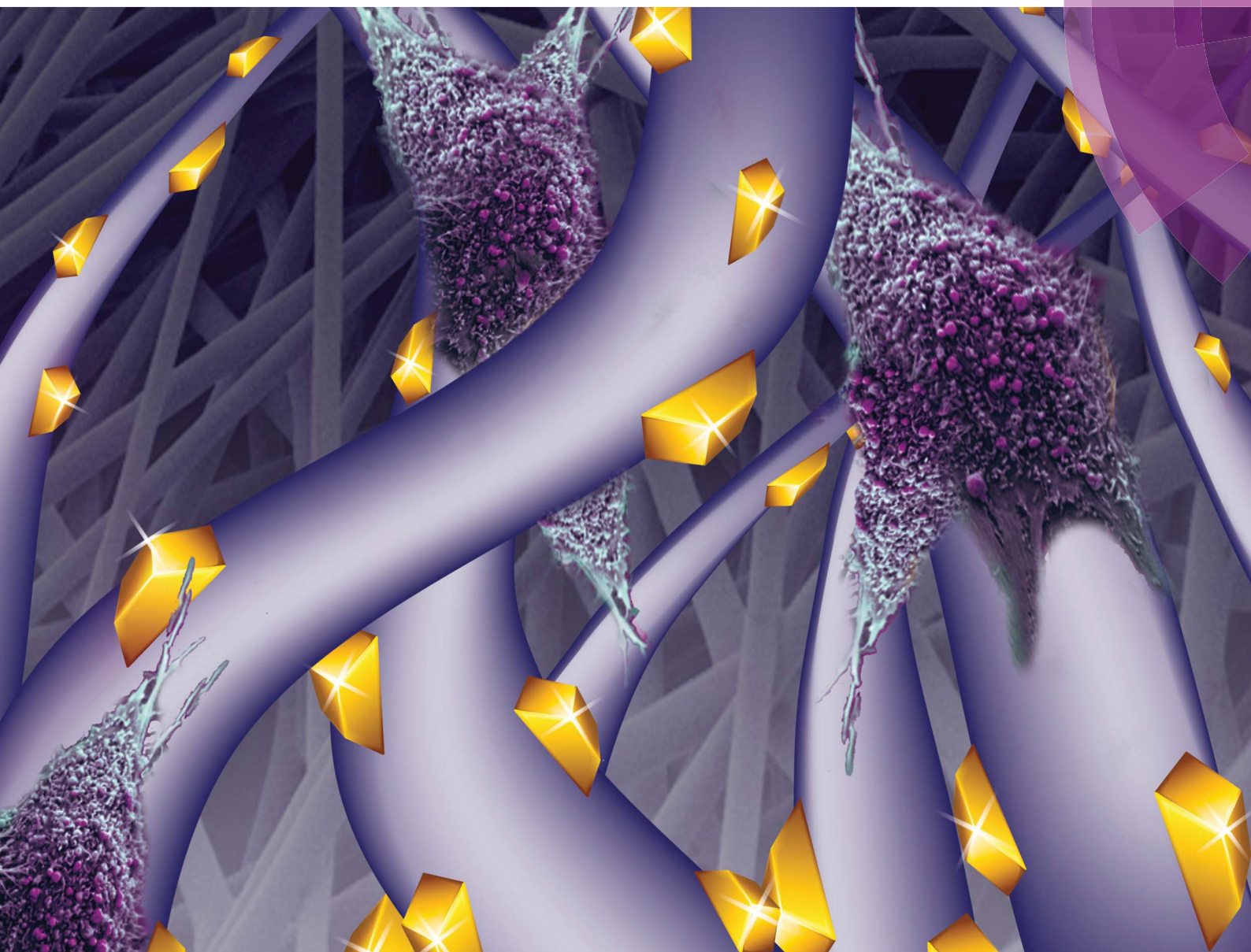


Nanoscale

www.rsc.org/nanoscale



ISSN 2040-3364



COMMUNICATION

Tal Dvir *et al.*

Coiled fiber scaffolds embedded with gold nanoparticles improve the performance of engineered cardiac tissues




 CrossMark
click for updates
Cite this: *Nanoscale*, 2014, 6, 9410Received 16th January 2014
Accepted 9th March 2014

DOI: 10.1039/c4nr00300d

www.rsc.org/nanoscale

Coiled fiber scaffolds embedded with gold nanoparticles improve the performance of engineered cardiac tissues†

Sharon Fleischer,^{†ab} Michal Shevach,^{†ab} Ron Feiner^{†ab} and Tal Dvir^{*abc}

Coiled perimysial fibers within the heart muscle provide it with the ability to contract and relax efficiently. Here, we report on a new nanocomposite scaffold for cardiac tissue engineering, integrating coiled electrospun fibers with gold nanoparticles. Cultivation of cardiac cells within the hybrid scaffolds promoted cell organization into elongated and aligned tissues generating a strong contraction force, high contraction rate and low excitation threshold.

Introduction

One of every three deaths in the United States is caused by cardiovascular diseases.¹ Myocardial infarction (MI) is a significant part of these diseases, and is associated with significant morbidity and mortality.² To date, strategies such as cell therapy, where cells are injected directly to the infarct, have been developed to repopulate the scar tissue with contracting cells.^{3,4} However, most of these strategies have shown limited success in sustaining the cells at the area of the infarct.^{5,6} Cardiac tissue engineering is a promising strategy for promoting heart regeneration.^{7–9} In this approach, cells are grown within three-dimensional (3D) biomaterials to promote their organization into contracting cardiac patches.^{10–15} Later on these patches can be implanted in the diseased heart to regain function.^{16,17} For successful cell assembly, integration and repair, the 3D scaffold supporting the cells should promote rapid electrical coupling between cardiac muscle cells and allow the formation of cell bundles to extend and contract efficiently.^{18,19} To improve cell–cell coupling at the electrical level

we have recently reported that cardiac cells can interact with each other through gold nanowires¹¹ or spherical nanoparticles.²⁰ These nanostructures were incorporated within 3D macroporous or electrospun scaffolds to form hybrid nanocomposite scaffolds. Cardiac tissues grown within these scaffolds exhibited anisotropic transfer of the electrical signals leading to higher contraction rates and stronger contraction forces.^{11,20}

Although synchronous contraction was observed throughout these engineered cardiac patches, the microenvironment in which the tissues were engineered lacked mechanical properties of the natural milieu. These properties are essential for efficient tissue contraction and relaxation.²³

The natural heart matrix contains a unique subpopulation of coiled perimysial fibers.²¹ These fibers stretch and re-coil with the heart muscle, providing it with unique mechanical properties crucial for its efficient and continuous contractions.^{21,22} Recently, we reported on the importance of recapitulating these fibers for engineering functional cardiac tissues.²³ Cardiac tissues grown within these coiled-fiber scaffolds exhibited stronger contraction forces, higher beating rates and lower excitation thresholds than tissues grown within straight fiber scaffolds.

Here we sought to further improve cardiac patch performances by integration of gold nanoparticles (AuNPs) ensuring anisotropic transfer of the electrical signals throughout engineered cardiac tissues, with coiled fiber scaffolds. Fig. 1 schematically illustrates the experimental process. Poly-

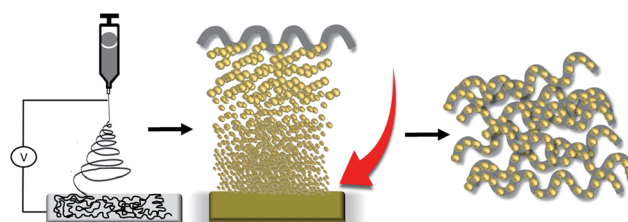


Fig. 1 Schematic representation of the study.

^aThe Laboratory for Tissue Engineering and Regenerative Medicine, Department of Molecular Microbiology and Biotechnology, George S. Wise Faculty of Life Sciences, Tel Aviv University, Tel Aviv 69978, Israel. E-mail: tdvir@post.tau.ac.il

^bThe Center for Nanoscience and Nanotechnology, Tel Aviv University, Tel Aviv 69978, Israel

^cDepartment of Materials Science and Engineering, Faculty of Engineering, Tel Aviv University, Tel Aviv 69978, Israel

† Electronic supplementary information (ESI) available. See DOI: 10.1039/c4nr00300d

‡ Equal contribution.

(ϵ -caprolactone) (PCL) was dissolved in a 1:1 ratio of dichloromethane (DCM) and dimethylformamide (DMF), and electrospun on a static collector to fabricate coiled fibers. The fibers were then placed in a VST e-beam evaporator and Au was deposited on their surface to create the nanocomposite coiled fiber scaffolds.

Inspired by the structure of natural coiled perimysial fibers (Fig. 2A), we synthetically fabricated similar coiled electrospun fibers (Fig. 2B). Scaffolds composed of such coiled fibers with diameters ranging between a few hundreds of nanometers to several micrometers exhibited an average pore area $>4000 \mu\text{m}^2$ (Fig. 2C and D).²³ We next sought to overcome the limited ability of the scaffolds to propagate the electrical signals between cultured cardiac cells by evaporating AuNPs with a nominal thickness of 10 nm onto the surface of the fibers. ESEM images revealed that AuNPs were homogeneously distributed on the surface of the fibers (Fig. 2E). Elemental mapping using energy dispersive X-ray spectroscopy (EDX) confirmed that the scaffolds were covered with AuNPs (Fig. 2F).

Recently it was reported that modification of silk electrospun fibers with AuNPs altered their mechanical properties.²⁴ To investigate the effect of the AuNPs on the coiled fibers, single fibers were electrospun on slides and the z-axis-Young's modulus of fibers with and without AuNPs was investigated using an atomic force microscope (AFM). Fig. 3A and B show the topography of fibers with and without AuNPs. While the pristine fibers are relatively smooth, the AuNPs are clearly seen on the surface of the modified fibers. This allows a relatively easy placement of the AFM tip on the AuNPs for measuring the mechanical properties of the composite fibers. As shown, the AuNPs significantly increased the elastic modulus of the fibers (Fig. 3B; $p = 0.008$). Measuring the fiber stiffness in the longitudinal direction by using a Lloyd mechanical tester revealed no change between the groups (data not shown).

Next, we investigated the potential of the AuNP-coiled fiber scaffolds (AuNP scaffolds) to induce cardiac cell assembly into a

mature tissue with morphological and biochemical hallmarks resembling those of the natural myocardium. We and others have previously shown that engineered cardiac tissue function can be improved by incorporation of gold nanostructures into macroporous scaffolds, hydrogels or straight fibers.^{11,20,25} In this study, we sought to explore the potential of AuNPs to improve the structural and functional assembly of cardiac tissues grown within coiled fiber scaffolds. Cardiac cells were isolated from neonatal rats and cultured for 7 days within pristine or AuNP scaffolds. On day 7, engineered cardiac tissues were stained for α -sarcomeric actinin, a marker associated with cardiac muscle contraction. Fig. 4A shows cardiac cells cultured within pristine scaffolds exhibiting limited cell spreading and a rounded morphology. Furthermore, massive cell-cell interactions were not observed and cardiac cell bundles were not formed. In contrast, cardiac cells cultured within AuNP scaffolds exhibited an aligned and elongated morphology with massive actinin striation (Fig. 4B). The cells organized into elongated and aligned cardiac-cell bundles, resembling the natural morphology of cell bundles in the myocardium.¹⁰ These results suggest the formation of a cardiac tissue with a strong contraction potential. Analysis of the cell area within the two types of scaffolds on days 3 and 7 revealed a significantly larger cell area in the AuNP scaffolds (Fig. 4C; $p = 0.004$ on day 3, and $p < 0.0001$ on day 7). Moreover, analysis of cell elongation (presented as the cell aspect ratio) revealed that on day 3 and 7 cardiac cells cultured within AuNP scaffolds had a significantly higher aspect ratio than those grown in pristine scaffolds (Fig. 4D; $p = 0.005$ on day 3, and $p = 0.01$ on day 7). Overall these results indicate that the AuNPs encouraged cardiac cell assembly into an organized and dense tissue with a strong and anisotropic contraction potential.

Finally, we were interested to assess the potency of AuNP scaffolds in inducing the assembly of a functional cardiac tissue. In an attempt to improve heart function after MI an engineered cardiac patch should be able to generate a strong

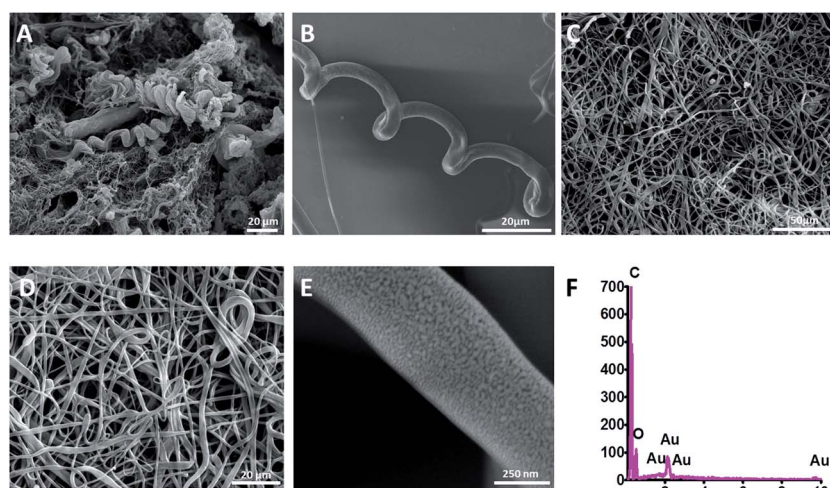


Fig. 2 Native and synthetic coiled fibers. (A) SEM image of the coiled perimysial fibers in a decellularized heart. (B) ESEM image of an electrospun coiled fiber embedded with AuNPs. (C and D) SEM images of coiled fiber scaffolds. (E) ESEM image of the AuNPs embedded on the synthetic fiber. (F) EDX spectrum of AuNP coiled fibers. Bars: (A), (B) and (D) – 20 μm , (C) – 50 μm , and (E) – 250 nm.

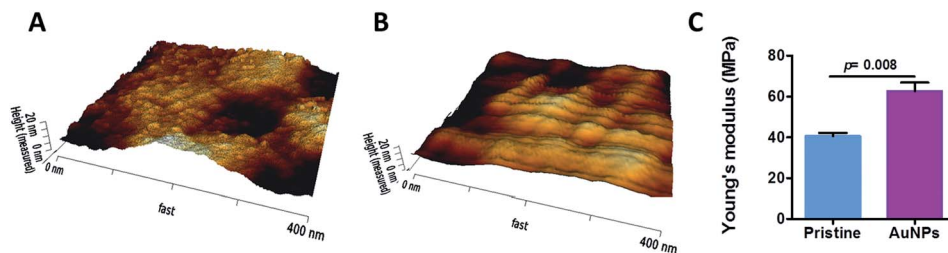


Fig. 3 Topography and mechanical properties by AFM. (A) Topography of a coiled fiber supplemented with AuNPs. (B) Topography of a non-modified coiled fiber. (C) Analysis of Young's modulus by AFM.

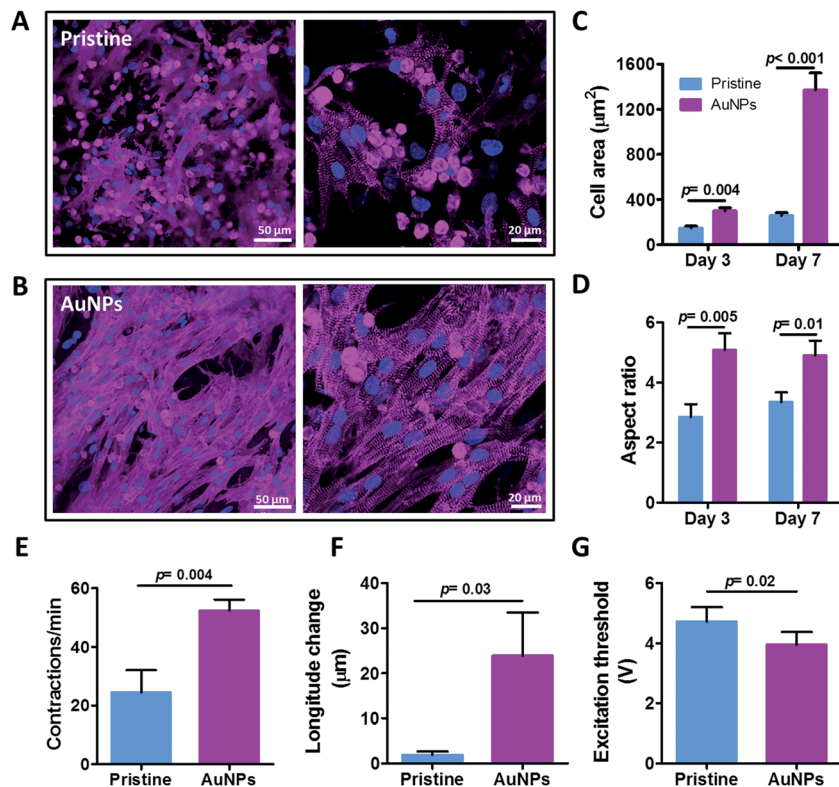


Fig. 4 Cardiac tissue organization and function. (A and B) Cardiac sarcomeric actinin immunostaining on day 7. Actinin – pink, nuclei – blue. (A) Cardiac tissue engineered within pristine scaffolds. (B) Cardiac tissue engineered within AuNP scaffolds. (C) Cardiomyocyte area on day 3 and 7. (D) Cardiomyocyte aspect ratio on days 3 and 7. (E–G) Engineered tissue function. (E) Contraction rate on day 7. (F) Longitude change of the cell constructs on day 7. (G) Excitation threshold (ET) on day 7. Bars: left and right figures – 50 μm and 20 μm, respectively.

contraction force.¹⁸ Analysis of tissue contraction rates revealed significantly higher rates in tissues cultured within the AuNP scaffolds as compared to pristine scaffolds (Fig. 4E, and ESI Movies 1 and 2;† $p = 0.004$). To evaluate the contraction force that the tissues can generate, the longitude change of the cardiac patches was measured on day 7. Cardiac tissues cultured within AuNP scaffolds generated significantly stronger contraction forces as compared to the tissues grown within the pristine scaffolds (Fig. 4F, and ESI Movies 1 and 2;† $p = 0.03$). Based on previous studies we hypothesized that AuNPs will induce superior cell electrical coupling, leading to synchronous contraction of the entire tissue.^{11,20} To investigate this, cardiac constructs were subjected to an external electrical field, increasing in increments of 0.1 V. We defined excitation

threshold as the minimum voltage needed to induce synchronous contractions of the entire patch at the defined frequency (higher than the normal contraction rate). Fig. 4G shows cardiac tissues grown within AuNP scaffolds reacting to significantly lower electrical fields compared to those grown in pristine scaffolds ($p = 0.02$). Overall, our results indicated the superior function of cardiac tissues cultured within coiled fiber scaffolds incorporated with AuNPs.

Conclusions

In this article we report on the incorporation of AuNPs into coiled fiber scaffolds for cardiac tissue engineering. The structure of the electrospun fibers resembled that of the coiled

perimysial fibers present in the native heart matrix, allowing proper contraction and relaxation of the myocardium. The addition of AuNPs to the scaffolds induced a quick formation of elongated and aligned cardiac tissues with a morphology resembling that of cardiac cell bundles *in vivo*. Furthermore, tissues engineered within AuNP-coiled fiber scaffolds exhibited superior function. We believe that the reported technology can be used for engineering cardiac tissues with superior functionality within various types of biomaterial scaffolds.

Experimental

Electrospinning

PCL (17.5% w/v, M_n 80 000, Sigma-Aldrich, St. Louis, MO) was dissolved in DCM and DMF in a ratio of 1 : 1. A syringe pump (Harvard apparatus, Holliston, MA) was used to deliver the polymer solution through a stainless steel 20G capillary at a rate of 0.5 mL h⁻¹. A high voltage power supply (Glassman high voltage Inc., Whitehouse Station, NJ) was used to apply a 17.5 kV potential between the capillary tip and the grounded aluminum collector placed 15 cm away. The obtained fibers were examined under a light microscope to verify the coiled morphology and then air-dried for 48–72 h to allow the residual solvent to evaporate.

Gold NP preparation

Scaffolds, or single electrospun fibers were mounted on a VST e-beam evaporator. Au films (10 nm thick) were prepared by evaporation of Au (99.999%) from a tungsten boat at $1-3 \times 10^{-6}$ torr at a deposition rate of 0.5 Å s⁻¹.

Topography and mechanical property measurements by AFM

Topography and mechanical property measurements were performed using a JPK research AFM (model NanoWizard III) in the force spectroscopy mode. We used NanoSensors, PPP-NCHR-50 scanning probe, resonance frequency range of 204–497 kHz, force constant range of 10–130 N m⁻¹.

Scanning electron microscopy

Coiled-fiber scaffolds. Scaffolds were mounted onto aluminum stubs with conductive paint and sputter-coated with an ultrathin (150 Å) layer of gold in a Polaron E 5100 coating apparatus. The samples were viewed under SEM (JEOL model JSM-840A) at an accelerating voltage of 25 kV.

AuNP coiled fibers. Fibers were imaged without additional coating using a Quanta 200 FEG Environmental Scanning Electron Microscope (ESEM) with a field-emission gun (FEG) electron source. Imaging was carried out under low vacuum with a high tension of 20 kV and a working distance of 7.3 mm.

Cardiac cell isolation, seeding and cultivation

Cardiac cells were isolated as previously described.²⁶ Briefly, left ventricles of 0–3 day old neonatal Sprague-Dawley rats were harvested and cells were isolated using 6 cycles (30 min each) of enzyme digestion with collagenase type II (95 U mL⁻¹;

Worthington, Lakewood, NJ) and pancreatin (0.6 mg mL⁻¹; Sigma-Aldrich) in Dulbecco's modified Eagle medium, (CaCl₂ · 2H₂O (1.8 mM), KCl (5.36 mM), MgSO₄ · 7H₂O (0.81 mM), NaCl (0.1 M), NaHCO₃ (0.44 mM), and NaH₂PO₄ (0.9 mM)). After each round of digestion cells were centrifuged (600 G, 5 min) and re-suspended in a culture medium composed of M-199 (Biological Industries, Beit-Haemek, Israel) supplemented with 0.6 mM CuSO₄ · 5H₂O, 0.5 mM ZnSO₄ · 7H₂O, 1.5 mM vitamin B12, 500 U mL⁻¹ penicillin and 100 mg mL⁻¹ streptomycin, and 0.5% (v/v) FBS. To enrich the cardiomyocytes population, cells were suspended in culture medium with 5% FBS and pre-plated twice (30 min). Then, the cells were counted and seeded on the scaffolds using a single droplet. The cell-seeded constructs were cultivated at 37 °C in a 5% carbon dioxide humidified incubator.

Immunostaining

Immunostaining was performed as previously described.²⁷ Cardiac cell constructs were fixed and permeabilized in 100% cold methanol for 10 min, washed three times with DMEM-based buffer and then blocked for 1 h at room temperature in DMEM-based buffer containing 2% FBS. The samples were then incubated with primary antibodies to detect α -sarcomeric actinin (1 : 750, Sigma-Aldrich), washed three times, and incubated for 1 h with Alexa Fluor 647 conjugated goat anti-mouse antibody (1 : 500; Jackson, West Grove, PA). For nuclei detection, the cells were incubated for 3 min with Hoechst 33258 (1 : 100; Sigma-Aldrich) and washed three times. Samples were visualized using a confocal microscope (Nikon Eclipse Ni).

Functional assessment

Contractions. Samples were filmed under a microscope (Nikon Eclipse TI, inverted) for functional assessments. Longitude change during tissue contraction was analyzed using image J (NIH). The contraction rate was counted. At least 5 samples from each group were used for analyses.

Excitation threshold. Cell constructs were placed in Tyrode's solution at 37 °C between two carbon electrode rods placed 1 cm apart in a Petri dish. Constructs were stimulated with 100 ms square pulses delivered at a rate of 2 Hz, starting with an amplitude of 1 V electrical field. The amplitude was increased by 0.1 V increments. The excitation threshold was defined as the voltage where the tissue construct started to contract synchronously at a frequency of 2 Hz.

Statistical analysis

Statistical analysis data are presented as means \pm SEM. Univariate differences between the pristine scaffold and AuNP scaffolds were assessed by Student's *t*-test. All analyses were performed using GraphPad Prism version 5.00 for Windows (GraphPad Software). *p* < 0.05 was considered significant.

Acknowledgements

T.D acknowledges support from the European Union FP7 program (Marie Curie, CIG), Alon Fellowship, the Israeli Science

Foundation, and the Nicholas and Elizabeth Slezak Super Center for Cardiac Research and Biomedical Engineering at Tel Aviv University.

References

- 1 A. S. Go, D. Mozaffarian, V. L. Roger, E. J. Benjamin, J. D. Berry, M. J. Blaha, *et al.*, Heart Disease and Stroke Statistics-2014 Update: A Report From the American Heart Association, *Circulation*, 2013.
- 2 A. S. Go, D. Mozaffarian, V. L. Roger, E. J. Benjamin, J. D. Berry, W. B. Borden, *et al.*, Executive summary: heart disease and stroke statistics-2013 update: a report from the American Heart Association, *Circulation*, 2013, **127**(1), 143–152.
- 3 A. R. Williams, K. E. Hatzistergos, B. Addicott, F. McCall, D. Carvalho, V. Suncion, *et al.*, Enhanced effect of combining human cardiac stem cells and bone marrow mesenchymal stem cells to reduce infarct size and to restore cardiac function after myocardial infarction, *Circulation*, 2013, **127**(2), 213–223.
- 4 R. Bolli, A. R. Chugh, D. D'Amario, J. H. Loughran, M. F. Stoddard, S. Ikram, *et al.*, Cardiac stem cells in patients with ischaemic cardiomyopathy (SCIPIO): initial results of a randomised phase 1 trial, *Lancet*, 2011, **378**(9806), 1847–1857.
- 5 S. Fleischer and T. Dvir, Tissue engineering on the nanoscale: lessons from the heart, *Curr. Opin. Biotechnol.*, 2013, **24**(4), 664–671.
- 6 J. Buikema, P. van der Meer, J. P. Sluijter and I. J. Domian, Engineering Myocardial Tissue: The Convergence of Stem Cells Biology and Tissue Engineering Technology, *Stem Cells*, 2013.
- 7 M. A. Laflamme and C. E. Murry, Heart regeneration, *Nature*, 2011, **473**(7347), 326–335.
- 8 G. Vunjak-Novakovic, N. Tandon, A. Godier, R. Maidhof, A. Marsano, T. P. Martens, *et al.*, Challenges in cardiac tissue engineering, *Tissue Eng., Part B*, 2010, **16**(2), 169–187.
- 9 T. Eschenhagen, A. Eder, I. Vollert and A. Hansen, Physiological aspects of cardiac tissue engineering, *Am. J. Physiol.: Heart Circ. Physiol.*, 2012, **303**(2), H133–H143.
- 10 T. Dvir, B. P. Timko, D. S. Kohane and R. Langer, Nanotechnological strategies for engineering complex tissues, *Nat. Nanotechnol.*, 2011, **6**(1), 13–22.
- 11 T. Dvir, B. P. Timko, M. D. Brigham, S. R. Naik, S. S. Karajanagi, O. Levy, *et al.*, Nanowired three-dimensional cardiac patches, *Nat. Nanotechnol.*, 2011, **6**(11), 720–725.
- 12 M. Radisic, H. Park, H. Shing, T. Consi, F. J. Schoen, R. Langer, *et al.*, Functional assembly of engineered myocardium by electrical stimulation of cardiac myocytes cultured on scaffolds, *Proc. Natl. Acad. Sci. U. S. A.*, 2004, **101**(52), 18129–18134.
- 13 Y. Sapir, O. Kryukov and S. Cohen, Integration of multiple cell-matrix interactions into alginate scaffolds for promoting cardiac tissue regeneration, *Biomaterials*, 2011, **32**(7), 1838–1847.
- 14 B. Liao, N. Christoforou, K. W. Leong and N. Bursac, Pluripotent stem cell-derived cardiac tissue patch with advanced structure and function, *Biomaterials*, 2011, **32**(35), 9180–9187.
- 15 G. C. Engelmayr Jr, M. Cheng, C. J. Bettinger, J. T. Borenstein, R. Langer and L. E. Freed, Accordion-like honeycombs for tissue engineering of cardiac anisotropy, *Nat. Mater.*, 2008, **7**(12), 1003–1010.
- 16 T. Dvir, A. Kedem, E. Ruvinov, O. Levy, I. Freeman, N. Landa, *et al.*, Prevascularization of cardiac patch on the omentum improves its therapeutic outcome, *Proc. Natl. Acad. Sci. U. S. A.*, 2009, **106**(35), 14990–14995.
- 17 W. H. Zimmermann, I. Melnychenko, G. Wasmeier, M. Didie, H. Naito, U. Nixdorff, *et al.*, Engineered heart tissue grafts improve systolic and diastolic function in infarcted rat hearts, *Nat. Med.*, 2006, **12**(4), 452–458.
- 18 R. K. Iyer, L. L. Chiu, L. A. Reis and M. Radisic, Engineered cardiac tissues, *Curr. Opin. Biotechnol.*, 2011, **22**(5), 706–714.
- 19 N. Bursac, Y. Loo, K. Leong and L. Tung, Novel anisotropic engineered cardiac tissues: studies of electrical propagation, *Biochem. Biophys. Res. Commun.*, 2007, **361**(4), 847–853.
- 20 M. Shevach, B. M. Maoz, R. Feiner, A. Shapira and T. Dvir, Nanoengineering gold particle composite fibers for cardiac tissue engineering, *J. Mater. Chem. B*, 2013, **1**(39), 5210–5217.
- 21 T. F. Robinson, M. A. Geraci, E. H. Sonnenblick and S. M. Factor, Coiled perimysial fibers of papillary muscle in rat heart: morphology, distribution, and changes in configuration, *Circ. Res.*, 1988, **63**(3), 577–592.
- 22 P. J. Hanley, A. A. Young, I. J. LeGrice, S. G. Edgar and D. S. Loiselle, 3-Dimensional configuration of perimysial collagen fibres in rat cardiac muscle at resting and extended sarcomere lengths, *J. Physiol.*, 1999, **517**(Pt 3), 831–837.
- 23 S. Fleischer, R. Feiner, A. Shapira, J. Ji, X. Sui, H. Daniel Wagner, *et al.*, Spring-like fibers for cardiac tissue engineering, *Biomaterials*, 2013, **34**(34), 8599–8606.
- 24 T. Cohen-Karni, K. J. Jeong, J. H. Tsui, G. Reznor, M. Mustata, M. Wanunu, *et al.*, Nanocomposite gold-silk nanofibers, *Nano Lett.*, 2012, **12**(10), 5403–5406.
- 25 J. O. You, M. Rafat, G. J. Ye and D. T. Auguste, Nanoengineering the heart: conductive scaffolds enhance connexin 43 expression, *Nano Lett.*, 2011, **11**(9), 3643–3648.
- 26 T. Dvir, N. Benishti, M. Shachar and S. Cohen, A novel perfusion bioreactor providing a homogenous milieu for tissue regeneration, *Tissue Eng.*, 2006, **12**(10), 2843–2852.
- 27 T. Dvir, O. Levy, M. Shachar, Y. Granot and S. Cohen, Activation of the ERK1/2 cascade via pulsatile interstitial fluid flow promotes cardiac tissue assembly, *Tissue Eng.*, 2007, **13**(9), 2185–2193.